Published in final edited form as:
Nat Immunol. 2013 September ; 14(9): 959–965. doi:10.1038/ni.2649.

Anti-apoptotic Mcl-1 is critical for the survival and niche-filling capacity of Foxp3$^+$ regulatory T cells

Wim Pierson[1,2], **Bénédicte Cauwe**[1,2], **Antonia Policheni**[3,4], **Susan M. Schlenner**[1,2], **Dean Franckaert**[1,2], **Julien Berges**[5,6], **Stephanie Humblet-Baron**[1,2], **Susann Schonefeldt**[1,2], **Marco J. Herold**[3,4], **David Hildeman**[7,8], **Andreas Strasser**[3,4], **Philippe Bouillet**[3,4], **Li-Fan Lu**[9], **Patrick Matthys**[10], **Antonio A. Freitas**[5,6], **Rita J. Luther**[11], **Casey T. Weaver**[11], **James Dooley**[1,2], **Daniel H. D. Gray**[3,4,*], and **Adrian Liston**[1,2,*]

[1]Autoimmune Genetics Laboratory, VIB, Leuven, Belgium

[2]Department of Microbiology and Immunology, University of Leuven, Leuven, Belgium

[3]The Walter and Eliza Hall Institute of Medical Research, Melbourne, Australia

[4]Department of Medical Biology, University of Melbourne, Melbourne, Australia

[5]Unité de Biologie des Populations Lymphocytaires, Department of Immunology, Institut Pasteur, Paris, France

[6]Centre national de la recherché scientifique, URA 1961, Paris, France

[7]Division of Immunobiology, University of Cincinnati College of Medicine, Cincinnati, Ohio, USA

[8]Children's Hospital Medical Center, Cincinnati, Ohio, USA

[9]Section of Molecular Biology, Division of Biological Sciences, University of California–San Diego, La Jolla, California, USA

[10]Laboratory of Immunobiology, Rega Institute, University of Leuven, Leuven, Belgium

[11]Department of Pathology, University of Alabama at Birmingham, Birmingham, Alabama, USA

Abstract

Foxp3$^+$ regulatory T (T_{reg}) cells are a crucial immunosuppressive population of CD4$^+$ T cells, yet the homeostatic processes and survival programs that maintain the T_{reg} cell pool are poorly understood. Here we report that peripheral T_{reg} cells markedly alter their proliferative and apoptotic rates to rapidly restore numerical deficit through an interleukin 2–dependent and costimulation-dependent process. By contrast, excess T_{reg} cells are removed by attrition, dependent on the Bim-initiated Bak- and Bax-dependent intrinsic apoptotic pathway. The antiapoptotic proteins Bcl-x_L and Bcl-2 were dispensable for survival of T_{reg} cells, whereas Mcl-1

Correspondence should be addressed to A.L. (adrian.liston@vib.be) or D.H.D.G. (dgray@wehi.edu.au).
*These authors contributed equally to this work.

Author Contributions

W.P., B.C., A.P., S.M.S., J.B., M.H., S.S., D.F., S.H.-B., L.L. and J.D. performed the experiments. D.H., A.S., P.B., R.J.L. and C.T.W. provided key reagents. S.M.S., A.A.F., P.M., J.D., D.H.D.G. and A.L. designed the study. W.P., D.H.D.G. and A.L. wrote the manuscript. All authors read and approved the manuscript.

The authors declare no competing financial interests.

was critical for survival of T_{reg} cells, and the loss of this antiapoptotic protein caused fatal autoimmunity. Together, these data define the active processes by which T_{reg} cells maintain homeostasis via critical survival pathways.

The expression of the transcription factor Foxp3 in T cells results in radical transcriptional rewiring[1] and the consequent functional differentiation of these cells into T_{reg} cells. The most profound effect is the switch from a proimmunity potential to a protolerance function that is essential for preventing fatal systemic autoimmunity[2]. In addition to this archetypal characteristic, the transcriptional rewiring also alters the basic cellular properties of T_{reg} cells, including differential reliance on cytokines[3,4] and T cell receptor (TCR) signaling[5] for homeostasis as well as an unusual anergic and apoptotic behavior *in vitro*. The size of the T_{reg} cell population is critical for immunological balance; even relatively minor modulation alters immunity[6]. Abnormally low numbers of T_{reg} cells have been observed in multiple autoimmune and inflammatory conditions[7], whereas high numbers of T_{reg} cells in the aged are thought to contribute to the partial immunosuppressed state[8,9]. In addition, T_{reg} cells are postulated to impede effective immunity against cancer[10], with expansion of T_{reg} cells after radiotherapy reported to limit lymphoma clearance[11]. Given the growing interest in manipulating T_{reg} cell numbers in clinical settings, there is a pressing need to understand the cellular and molecular biology of T_{reg} cell homeostasis.

Apoptotic cell death is a major regulator of hematopoietic cell homeostasis[12]. In vertebrates, two distinct, but ultimately converging, pathways control apoptosis. The ‘extrinsic’ or ‘death receptor’ pathway is initiated by ligation of cell-surface death domain–containing members of the TNF-receptor family. The ‘intrinsic’ or ‘mitochondrial’ pathway is initiated by cellular stressors that alter the balance between proapoptotic and antiapoptotic members of the Bcl-2 family of proteins, culminating in the activation of Bax and Bak, and subsequent release of apoptogenic factors from mitochondria[13]. The two pathways converge upon the activation of ‘executioner’ caspases that demolish the cell. In the intrinsic apoptosis pathway, activation of Bax or Bak is the ‘point of no return’ and thus requires tight regulation. The prosurvival proteins Bcl-2, Bcl-xL, Mcl-1, A1 and Bcl-w restrain the activation of Bax and Bak, whereas proapoptotic proteins containing only the Bcl-2 homology domain BH3 (the so-called BH3-only proteins: Bim, Puma, Bid, Bmf, Bad, Noxa, Bik and Hrk) inhibit the prosurvival members and are essential for initiation of apoptosis signaling[14]. The relative importance of each of these proteins varies among different cell types or cytotoxic stimuli and therefore has to be evaluated on a case-by-case basis.

In this study we took advantage of the location of *Foxp3* on the X chromosome and the effect of X inactivation on a diphtheria toxin (DT) receptor knock-in construct to study the dynamics of T_{reg} cell responses to homeostatic perturbation in a highly controlled manner. We found that modulation of the T_{reg} cell population created a TCR costimulation-dependent and IL-2–dependent feedback loop, which increased proliferation of T_{reg} cells and diminished apoptosis to drive rapid restoration of T_{reg} cell numbers. Furthermore, we found that the Bak- and Bax-dependent intrinsic apoptotic pathway naturally limited the T_{reg} cell population, with T_{reg} cell accumulation observed in absence of Bak and Bax. Prosurvival Bcl-2 family member Mcl-1 safeguarded the survival of T_{reg} cells; deletion of

Mcl-1 caused a rapid loss of T_{reg} cells and onset of fatal autoimmunity. Mcl-1 expression is regulated by interleukin 2 (IL-2), which increased *Mcl1* transcription during the T_{reg} expansion phase after *in vivo* depletion. Finally, the BH3-only protein, Bim, is the primary antagonist of Mcl-1 in T_{reg} cells, as conditional deletion of Bim led to accumulation of excess T_{reg} cells, as observed with loss of Bak and Bax.

RESULTS

T_{reg} cells exhibit IL-2–dependent niche-filling behavior

To determine the homeostatic characteristics of T_{reg} cells, we compared the proliferative behavior of Foxp3$^+$ T_{reg} cells in 5-bromodeoxyuridine (BrdU) labeling experiments. In contrast to prior *in vitro* studies that characterized T_{reg} cells as semianergic, quiescent cells, we found that T_{reg} cells proliferated at a substantially faster rate than conventional T cells (CD4$^+$ or CD8$^+$) *in vivo*, with ~50% of the population having undergone proliferation within a 10-d window in unmanipulated hosts during homeostatic conditions (Supplementary Fig. 1). As these results suggest a highly dynamic yet stable population, we developed a 50% depletion system to examine responses to such perturbations in the T_{reg} cell niche using two different Foxp3 constructs. The first was *Thy1* (Thy1.1 variant) and the second was human *HBEGF* (diphtheria toxin receptor; DTR), each knocked into the *Foxp3* locus on the X chromosome. Female mice heterozygous for the *Foxp3*$^{Thy1.1}$ and *Foxp3*^{DTR} alleles (*Foxp3*$^{Thy1.1/DTR}$ mice) have two distinct populations of T_{reg} cells due to random X inactivation of *Foxp3* alleles. Half express the marker Thy1.1, and the other half express DTR. Non-T_{reg} cells express neither marker. Upon injection of DT, the DTR$^+$ T_{reg} cells will be rapidly eliminated and the response of the DTR$^-$Thy1.1$^+$ compartment to this 50% drop in total T_{reg} cell numbers can be tracked. An additional advantage of this system is that the use of Thy1.1 to mark untouched T_{reg} cells circumvents the difficulties in measuring apoptosis caused by the cleavage of Foxp3 by activated caspases (Supplementary Fig. 2). DT addition efficiently eliminated DTR$^+$ T_{reg} cells, but the overall proportion of Foxp3$^+$ cells was rapidly restored by the expansion of DTR$^-$Thy1.1$^+$ T_{reg} cells (Fig. 1a). The six fold increase in the number of Thy1.1$^+$ T_{reg} cells by day 5 caused an initial overshoot of ~200% in total T_{reg} cells, followed by a slow decline to basal levels (Fig. 1a and Supplementary Fig. 3). During the niche-filling process, proliferation rate of Thy1.1$^+$ T_{reg} cells increased, with the percentage of cells expressing the cell cycle protein Ki67 increasing from ~20% to ~70% (Fig. 1b). At the same time, the apoptosis rate of Thy1.1$^+$ T_{reg} cells decreased from ~40% to ~20% active caspase-3$^+$ (Fig. 1c). We found no evidence of any substantial contribution to the peripheral homeostasis of T_{reg} cells by recent thymic emigrants (tracked using a *Rag2-GFP* transgene or comparison to thymectomized mice; Supplementary Fig. 3h–j) or peripheral conversion of conventional T cells into T_{reg} cells, as this mechanism would have resulted in equal contribution by DTR$^+$ and Thy1.1$^+$ T_{reg} cells (the injected DT is cleared within hours). Therefore, we conclude that the expansion of existing T_{reg} cells must be the major driver of niche-filling in the 50% depletion system.

We observed an increase in effector-memory CD44^{hi}CD62L^{lo}CD4$^+$ T cells after partial depletion of T_{reg} cells (Supplementary Fig. 3); therefore, we determined whether T_{reg} cell niche-filling depended upon activation of T cells. Costimulatory blockade with a soluble

CTLA4-immunoglobulin fusion protein (CTLA4-Ig) to prevent activation of T cells negated restoration of T_{reg} cell numbers after partial depletion (Fig. 1d), consistent with a requirement for activation of conventional T cells (although this experiment does not rule out a T_{reg} cell–intrinsic requirement for costimulation). To test the role of dendritic cells (DCs) in this process, Itgax-Cre (CD11c-Cre) transgenic mice were crossed to *Rosa26-^{fl}stop^{fl}-DTR* (stop sequence flanked by LoxP-sites) knock-in mice to allow depletion of DCs via injection of DT. Depletion of dendritic cells (DCs) in *Foxp3$^{DTR/+}$* CD11c-Cre *Rosa26-^{fl}stop^{fl}-DTR* mice simultaneous with partial depletion of T_{reg} cells did not alter niche-filling kinetics (Supplementary Fig. 4), indicating that residual DCs or an alternate costimulation source is sufficient. Synchronous with T_{reg} cell niche-filling was an increase in plasma IL-2 levels and downregulation of the high-affinity subunit of the IL-2 receptor, CD25, by T_{reg} cells (Fig. 1e). The primary shift in CD25 expression was from CD25^{hi} to CD25^{int}, a change associated with increased proliferation (Supplementary Fig. 4), identifying IL-2 as a potential mediator of feedback from activation of conventional T cells to T_{reg} cells. To determine the source of IL-2 in this context, we generated mice with a bacterial artificial chromosome (BAC) transgenic *Thy1* (Thy1.1 variant) reporter of IL-2 production (unpublished data, RJ Luther and CT Weaver and crossed it onto the *Foxp3$^{DTR/+}$* background to track IL-2 production during 50% T_{reg} cell depletion. The numbers of IL-2–expressing conventional CD4^{+} T cells paralleled T_{reg} cell expansion kinetics (Fig. 1f). Accordingly, antibody-mediated IL-2 blockade in *Foxp3$^{Thy1.1/DTR}$* mice during the 50% T_{reg} cell depletion impaired niche-filling by partially inhibiting the greater proliferation rate and by completely blocking the decrease in apoptosis in the remaining T_{reg} cells (Fig. 1g–i). By contrast, short-term neutralization of IL-2 had little effect in the mice not treated with DT (data not shown), which may suggest that the low to undetectable baseline amounts of IL-2 have little effect on the default proliferative or apoptotic characteristics of T_{reg} cells, whereas the greater amount of IL-2 after perturbation drives substantial changes. The partial nature of the anti–IL-2 treatment may be due to the inability of the blocking antibody to completely inhibit this paracrine factor or may indicate that other factors can drive proliferation of T_{reg} cells during homeostatic expansion (Fig. 1h). Nevertheless, IL-2 was directly responsible for the altered apoptotic rate in T_{reg} cells (Fig. 1i), inhibition of which substantially blunts T_{reg} cell homeostatic expansion (Fig. 1g). Collectively, these data demonstrate that T_{reg} cells actively maintained homeostasis by swiftly responding to partial insufficiency via a feedback loop involving activation of conventional T cells, greater IL-2 production and altered T_{reg} cell proliferation and apoptosis.

Peripheral T_{reg} cell number is constrained by apoptosis

The cellular dynamics of T_{reg} cells after ablation highlighted the potential importance of T_{reg} cell apoptosis during two phases, namely during the expansion phase, when apoptosis was decreased, and during the contraction phase, when apoptosis mediated the decline in numbers. Conversely, proliferation rates when there was a surplus of T_{reg} cells did not drop below baseline at homeostasis (Fig. 1b), and we found no evidence for ‘deconversion’ of excess T_{reg} cells into conventional T cells when we used a fate-mapping tracker in *Foxp3$^{Cre/DTR}$ Rosa26-^{fl}stop^{fl}-YFP*(stop sequence flanked by LoxP-sites) mice (Supplementary Fig. 3k). Despite this (indirect) evidence for modulation of apoptosis being crucial for homeostasis of T_{reg} cells, defects in the ‘death receptor’ pathway have not been

associated with increases in T_{reg} cell numbers[15,16]. By contrast, the marked expansion of T_{reg} cells observed in mice lacking the proapoptotic proteins Bax and Bak, or those lacking the BH3-only protein Bim, implicates the intrinsic pathway of apoptosis in regulating numbers of T_{reg} cells[4,17], although these studies could not distinguish greater conversion into the T_{reg} cell lineage because of defective thymocyte deletion from elevated peripheral homeostasis. To analyze the impact of the intrinsic pathway of apoptosis specifically on peripheral T_{reg} cell homeostasis, we generated *Foxp3*^{Cre} *Bak1*$^{-/-}$ *Bax*$^{fl/fl}$ mice. Owing to the redundancy of Bak and Bax[18], this resulted in a T_{reg} cell–specific knockout of the entire intrinsic apoptotic pathway. These mice exhibited normal thymic development of T_{reg} cells (Supplementary Fig. 5), but peripheral accumulation of Foxp3$^+$ T_{reg} cells to twice the normal numbers (Fig. 2). This accumulation was not due to excess proliferation (turnover was lower; Fig. 2a). These data indicate that the intrinsic pathway of apoptosis is a critical regulator of peripheral T_{reg} cell homeostasis.

T_{reg} cells require Mcl-1 for survival

Bak and Bax activation is tightly regulated by prosurvival members of the Bcl-2 family, of which Bcl-2, Bcl-x_L and Mcl-1 have been reported to be expressed in T_{reg} cells[1]. The leading prosurvival candidate for maintaining T_{reg} cell survival was Bcl-2, because of the dynamic expression of Bcl-2 observed in T_{reg} cells[19–21] and the T_{reg} cell accumulation that occurs in mice with forced Bcl-2 overexpression[21]. However, lethally irradiated mice reconstituted with a 50:50 mixture of C57BL/6.Ly5.1:*Bcl2*$^{-/-}$ hematopoietic precursors exhibited a normal proportion of T_{reg} cells derived from the *Bcl2*-deficient compartment, demonstrating that Bcl-2 is dispensable for their survival (Fig. 3a,b). We could not analyze the second candidate, Bcl-x_L, using conventional knockouts (and hematopoietic reconstitution), as it is required for cell survival at the CD4$^+$CD8$^+$ thymocyte stage[22,23]. We therefore created mice with T_{reg} cell–specific ablation of Bcl-x_L by crossing a *Foxp3*^{Cre} strain[24] with *Bcl2l1*^{fl} mice[25]. The resulting *Foxp3*^{Cre}*Bcl2l1*$^{fl/fl}$ mice had normal numbers of T_{reg} cells in both the thymus and periphery with no obvious immunological or pathological phenotype, demonstrating no role for this anti-apoptotic protein in homeostasis of T_{reg} cells (Fig. 3c,d).

To investigate a potential role of Mcl-1 in regulating T_{reg} cell apoptosis, we used a huCD4 reporter of Mcl-1 expression. The *Mcl1*^{fl} allele we used was designed to bring a human *CD4* reporter in-frame after Cre recombinase–mediated excision[26]. When we crossed *Mcl1*$^{fl/+}$ mice to *Cd127*^{Cre} knock-in mice[27], expression of Cre recombinase in early lymphoid progenitors resulted in recombination of the *Mcl1*^{fl} allele in the entire lineage, allowing for tracking of *Mcl1* transcription in all T cell subsets using the huCD4 reporter, while maintaining their survival with the wild-type *Mcl1* allele (that is, the genotype becomes *Mcl1*$^{huCD4/+}$ in the T cell lineage). This strategy allows the relative quantification of Mcl-1 expression in all T cell subsets with a greater dynamic range than previous profiling[28]. During thymic development, Mcl-1 reporter expression peaked at the DP stage, before an ~80% decrease in conventional CD4$^+$CD8$^-$ thymocytes (Fig. 4a). In contrast to conventional CD4$^+$CD8$^-$ cells, Foxp3$^+$CD4$^+$CD8$^-$ cells maintained elevated Mcl-1 reporter expression (Fig. 4a), and likewise peripheral T_{reg} cells expressed the Mcl-1 reporter at ~50% higher levels than conventional T cells (Fig. 4b,c). To assess the function of Mcl-1 in T_{reg} cells,

while circumventing the impact of its loss on the early thymocyte stage[29], we created mice with T_{reg} cell–specific deletion of *Mcl1*. In contrast to the redundancy of Bcl-2 and Bcl-x_L in survival of T_{reg} cells, we found that Mcl-1 was essential. *Foxp3^{Cre}Mcl1$^{fl/fl}$* mice succumbed to a fatal immunopathology, surviving to only 4–8 weeks of age (Fig. 4d,e). Pathology was associated with immunological dysregulation, inflammatory infiltrate, hyper-IgE (100 times normal levels), elevated amounts of antibodies to dsDNA, abnormally high proliferation of $CD8^+$ T cells, greater activation of $CD4^+$ T cells and spontaneous differentiation into T_H1, T_H2 and T_H17 effector cells (Fig. 4f–i, Supplementary Fig. 6 and data not shown), all hallmarks of the Foxp3-deficient scurfy phenotype.

In young *Foxp3^{Cre}Mcl1$^{fl/fl}$* mice, thymic T_{reg} cell development was relatively undisturbed and initially there was only a ~60% decrease in peripheral T_{reg} cells (Supplementary Fig. 6). However, unlike the *Foxp3$^{Thy1.1/DTR}$* model, this T_{reg} cell deficit could not be corrected by peripheral expansion in *Foxp3^{Cre}Mcl1$^{fl/fl}$* mice, with an additional decrease in T_{reg} cell numbers observed (Fig. 5a). Loss of Mcl-1–deficient T_{reg} cells was even more extreme in a competitive environment (Supplementary Fig. 7). Nevertheless, the deficit-sensing mechanism appeared intact, as the remaining T_{reg} cells in *Foxp3^{Cre}Mcl1$^{fl/fl}$* mice demonstrated a compensatory increase in proliferation (Fig. 5b). We observed no evidence of an outgrowth of T_{reg} cells with intact *Mcl1*, nor *Mcl1* excision in $Foxp3^-$ cells, using the *huCD4* reporter expressed only when *Mcl1* is excised (Fig. 5c). To measure the kinetics of T_{reg} cell loss after *Mcl1* ablation, we generated mixed hematopoietic chimeras with 50% Ly5.1 congenically labeled bone-marrow and 50% Ly5.2 labeled bone-marrow bearing a tamoxifen-inducible *CreERT2* and *loxP*-flanked (floxed) alleles of either *Mcl-1* or *Bcl2l1*. After reconstitution, we induced inducible knockout in a competitive context by oral gavage with tamoxifen. Punctual deletion of *Mcl1*, but not *Bcl2l1*, in this system caused T_{reg} cell numbers to collapse within 2 d (Fig. 5d,e), revealing an acute necessity for Mcl-1 in survival of T_{reg} cells.

Regulation of Mcl-1 in T_{reg} cells by Bim and IL-2

The importance of Mcl-1 expression for T_{reg} cell survival suggested that regulation of Mcl-1 may be important in setting the homeostatic balance of T_{reg} cells. Several of the proapoptotic BH3-only members of the Bcl-2 family can overcome the prosurvival function of Mcl-1 and thereby initiate apoptosis[30]; however, elevated numbers of T_{reg} cells have been observed only in Bim-deficient mice[4,17,19,21]. In these mice with germ-line deletion of *Bcl2l11*, this effect has been ascribed to additional T cells entering the T_{reg} cell lineage because of defective negative selection[17], and secondary effects owing to low-grade inflammation[31]. To circumvent these issues, we generated mice bearing a floxed *Bcl2l11* allele and crossed them with *Foxp3^{Cre}* mice to create a T_{reg} cell–specific deletion of *Bcl2l11*, where Bim is lost only after T_{reg} cell development. The *Foxp3^{Cre}Bcl2l11$^{fl/fl}$* mice exhibited normal thymic differentiation, with substantial peripheral expansion of $Foxp3^+$ T_{reg} cells (Fig. 6a,b). Notably, the scale of peripheral T_{reg} cell expansion expansion in *Foxp3^{Cre} Bcl2l11$^{fl/fl}$* mice was not as great as that observed in *Foxp3^{Cre} Bak$^{-/-}$ Bax$^{fl/fl}$* mice (Fig. 2a,b), indicating that, although Bim is the primary initiator of homeostatic T_{reg} cell apoptosis, additional BH3-only proteins (for example, Puma[32]) may have additional roles. In addition to the negative regulation of Mcl-1 by Bim, the IL-2–dependent decrease in

apoptosis during niche-filling (Fig. 1i) suggested that IL-2 might act as a positive regulator of Mcl-1. *In vitro* we observed that stimulation of T_{reg} cells with IL-2 increased the amount of Mcl-1 protein (Fig. 6c). We therefore crossed the *Cd127*^{Cre}*Mcl1*$^{huCD4/+}$ reporter system (described above) to the *Foxp3*$^{DTR/+}$ partial depletion system, to determine whether the greater availability of IL-2 during expansion of T_{reg} cells (Fig. 1) was linked to *in vivo* changes in expression of Mcl-1. We observed a rapid increase in Mcl-1 reporter expression in T_{reg} cells after partial depletion (Fig. 6d), coinciding with the IL-2–dependent decrease in apoptosis. To directly test the ability of IL-2 to induce expression of Mcl-1 *in vivo*, we injected Mcl-1 reporter mice (*Cd127*^{Cre}*Mcl1*$^{huCD4/+}$) with complexes of IL-2 and antibody to IL-2 (IL-2–anti-IL-2), which (as previously reported[33]) caused a rapid expansion of Foxp3$^+$ T_{reg} cells, with a twofold increase in the peripheral blood by day 2 (Fig. 6e). Accompanying this increase in Foxp3$^+$ T_{reg} cells was an increase in huCD4 expression (reporter for *Mcl-1* transcription) in T_{reg} cells, whereas conventional CD4$^+$ and CD8$^+$ T cells exhibited no change in huCD4 expression (Fig. 6f). Together, these results demonstrate that IL-2 regulates expression of Mcl-1 *in vitro* and *in vivo*, indicating a direct pathway in T_{reg} cells from greater availability of IL-2 availability to greater expression of Mcl-1 (and perhaps lower Bim expression; data not shown), less apoptosis and subsequent peripheral expansion (Supplementary Fig. 8).

DISCUSSION

Far from being the semianergic lineage first described in *in vitro* experiments, Foxp3$^+$ T_{reg} cells were highly dynamic and responsive in our experiments *in vivo*. Although entry into the Foxp3$^+$ lineage is a gated event[34], peripheral proliferation and apoptosis are the primary determinants of compartment size, with ~50% of the population having undergone proliferation every 10 d under homeostatic conditions. Several explanations present themselves for the necessity of a high turnover of the T_{reg} cell pool. First, chronic proliferation caused by TCR stimulation via self-antigen stimulation[35] may necessitate compensatory apoptosis; second, a proapoptotic effect of Foxp3 expression leads to greater basal apoptosis levels in T_{reg} cells[36], which may require compensatory proliferation; or third, high turnover itself may be required for sufficient regulatory function[37]. Assessment of T_{reg} cell responsiveness to perturbations from this basal state requires both swift contraction and a mechanism to leave the remaining cells unaffected. The natural chimeric state of female *Foxp3*$^{Thy1.1/DTR}$ mice used here fulfills both of these conditions, unlike models which rely on partial antibody-mediated depletion[38] or escape of abnormal DT-resistant T_{reg} cell clones[39]. This approach revealed a much more rapid and dynamic T_{reg} cell response to perturbation than that demonstrated in previous models[38,39], characterized by promptly increased proliferation with concomitant decrease in apoptosis. Furthermore, this system revealed an ‘overfilling’ effect followed by the slower attrition of T_{reg} cells via apoptosis to re-establish homeostatic levels. The contrast between rapid expansion in the face of T_{reg} cell deficiency and gradual contraction during T_{reg} cell excess is commensurate with the more severe physiological consequences of suboptimal immune suppression. In the range of induced variation studied here, modulation of the proliferation to apoptosis balance was sufficient to drive homeostatic correction, with any substantial involvement of thymic production, peripheral conversion or ‘de-conversion’ all excluded through experiments

under these conditions. While these processes are capable of rapidly restoring T_{reg} cell numbers, an implication of this heavy reliance on remaining T_{reg} cell expansion (as opposed to production of new T_{reg} cells) is that repeated episodes of partial T_{reg} cell deficiency may narrow the diversity of the TCR repertoire in the restored T_{reg} cell pool. The extent of any TCR repertoire restriction is unknown, but may be substantial in aged individuals due to periodic T_{reg} cell contraction and expansion, in addition to the stochastic loss of diversity due to the high baseline rates of T_{reg} cell proliferation and apoptosis.

Dissection of the molecular mediators of T_{reg} cell homeostatic responsiveness revealed how well-known participants in T_{reg} cell biology modify previously unappreciated survival pathways. We found a direct correlation between modulation of T_{reg} cell numbers and production of IL-2 by conventional T cells in a costimulation-dependent manner. Elevated expression of IL-2 by conventional T cells occurs before the attainment of a typical activated cell-surface profile, a phenomenon that may be related to the lower threshold of TCR signaling required for cytokine production[40] and which may serve to shorten the time lag of T_{reg} cell expansion in response to depletion. Consistent with previous reports identifying the importance of IL-2 for T_{reg} cells[35], blockade of IL-2 blunted the homeostatic rebound after 50% T_{reg} cell depletion, playing an essential role in the transient decrease in T_{reg} cell apoptosis and a significant role in the boost to proliferation. The reliance of the T_{reg} cell homeostatic feedback circuit on an inducible cytokine lies in stark contrast to the homeostatic feedback loops of B cells and non-regulatory T cells mediated by the cytokines, BAFF[41] and IL-7 (ref. 42), respectively, which are not made by activated T cells but constitutively produced by stromal cells[43,44]. Notably, a feature of such static consumption-based homeostatic systems is that only numerical, rather than functional, sufficiency is selected for. In the T_{reg} cell homeostatic system described here, by contrast, the dynamic production of IL-2 in response to $Foxp3^+$ regulatory T cell numbers makes the niche dependent on regulatory T cell function (that is, restraining improper T cell activation) as opposed to merely numerical sufficiency. It is predicted that such a homeostatic model will prove to show greater robustness when challenged by variation in the efficiency of T_{reg} cell suppression, as demonstrated by the increase in T_{reg} cell numbers in several models of impaired function[45,46].

A previously unappreciated key feature of the T_{reg} cell homeostatic feedback loops described here is the central role for apoptosis in regulating T_{reg} cell numbers. Expansion of T_{reg} cells during numerical deficit was accompanied by an IL-2–dependent suspension of apoptosis, while contraction during surplus involved apoptotic processes. Accordingly, T_{reg} cell–specific ablation of the intrinsic apoptosis pathway provoked the accumulation of surplus T_{reg} cells. Our approach of systematic assessing pro-survival members of the intrinsic apoptosis pathway revealed that Bcl-2 and Bcl-x_L were redundant, in contrast to prior supposition[17,19–21], while Mcl-1 was essential for T_{reg} cell survival. Furthermore, Mcl-1 appears to represent a rheostat for controlling the T_{reg} cell homeostatic niche, with positive regulation via IL-2 and antagonism by Bim during homeostatic perturbation. This role of the Mcl-1 and Bim axis in driving the return of T_{reg} cells to homeostatic levels represents a potential intervention point for therapeutic manipulation.

Online Methods

Mice

Bak$^{-/-}$ (ref. 18), *Bax*$^{fl/fl}$ (ref. 47), *Bcl-x(Bcl2l1)*$^{fl/fl}$ (ref. 25), *Bim(Bcl2l11)*$^{fl/fl}$ (ref. X), CD11c-Cre-Tg (ref. 48), CD127-Cre-Tg (ref. 27), *Foxp3*^{GFP} (ref. 49), *Foxp3*^{YFPCre} (ref. 24), *Foxp3*$^{Thy1.1}$ (ref. 50), IL-2.BAC-Thy1.1 mice (manuscript in preparation, RJ Luther and CT Weaver), *Mcl1*$^{fl/fl}$[26], *Rag2*$^{-/-}$ (ref. 51), Rag2GFP-Tg (ref. 52), *Rosa26-*^{fl}*stop*^{fl}*-YFP* (ref. 53), *Rosa26-*^{fl}*stop*^{fl}*-DTR* (ref. 54) and Rosa26$^{Cre\text{-}ERT2}$ (ref. 55) mice were all generated on, or backcrossed to, the C57BL/6 background. *Foxp3*^{DTR} mice[56] were backcrossed to the C57BL/6.Ly5.1 background. Experimental mice were housed under specific pathogen–free conditions. Disease development was monitored by frequent observation and post-mortem analysis. Cohorts of mice for the survival test were removed from the study at death or when veterinary advice indicated likely death within 48 h. All experiments were approved by the University of Leuven animal ethics committee or the WEHI animal ethics committee. Histological examination was performed by Histology Consultation Services and pathology reports were generated by BioGenetics.

Design of animal experiments

All endpoint experiments used 3 or more mice of the specified genotypes and age-range to enable statistical comparisons. Mice were assigned to groups based on a semi-randomization process that included a post-randomization reassignment to ensure equal age-sex distribution within groups. Investigators performing experiments were only aware of mouse ID numbers, not genotype. Genotypes were revealed only upon analysis.

Foxp3$^{DTR/Thy1.1}$ heterozygous females, 6–8 weeks of age, were injected intraperitoneally with a dose of 50 μg/kg of DT (Sigma-Aldrich) diluted in saline on days 0 and 1 (for CD11c depletion, on days 0, 1, 2 and 3) of the experiment. A daily dose of 50 μg of IL-2–neutralizing antibody (S4B6) or IgG2a isotype-matched control antibody (eBR2a, eBioscience) was administered intraperitoneally starting on the day of the first DT injection. CTLA4-Ig (abatacept, Bristol-Myers Squibb) was injected intraperitoneally (25 mg/kg) on days 0, 2 and 4.

Cd127^{Cre} *Mcl1*$^{wt/fl\text{-}huCD4}$ female mice, 6–8 weeks of age, were injected intraperitoneally with IL-2 complex at a dose of 16.5 μg/mouse per day. IL-2 complex was generated by mixing mouse recombinant IL-2 (eBioscience) with anti-mouse IL-2 antibody (JES6-1A12, eBioscience) at a 1:10 ratio, and was injected intraperitoneally at a dose of 16.5 μg/mouse per day, as per the published protocol[57].

Bone-marrow chimeric experiments were performed using recipient C57BL/6 *Rag2*$^{-/-}$ female mice sub-lethally irradiated with 9.5Gy at 8–12 weeks of age and reconstituted within 24 h using an intravenous injection with a total of 2×10^6 hematopoietic cells from bone marrow donors. Chimeric mice were analyzed at or after 6 weeks after reconstitution. For inducible deletion of *Bcl-x* or *Mcl1*, chimeric mice were given two doses of 200 mg/kg of tamoxifen (Sigma, T5648) via oral gavage on days 0 and 1.

BrdU exposure was initiated in C57BL/6 male mice, 6–8 weeks of age, via an intraperitoneal injection of 100 μg/100 μl BrdU (Sigma). A subset of mice were additionally given continuous exposure to 8 mg/ml BrdU in the drinking water, changed daily.

Flow cytometry

Leukocytes from peripheral blood, thymus, spleen or lymph nodes were analyzed using the following antibodies: anti-BrdU-APC (1/50) (B44, BD), anti-CD25-PECy7(1/300) (PC61.5), anti-CD25-PE (1/300) (BD), anti-CD4-APC-H7 (1/250) (GK1.5, BD), anti-CD4-PerCP (1/200) (GK1.5, BioLegend), anti-huCD4-PE (1/50) (OKT4, BD), anti-CD4-PE (1/200) (GK1.5), anti-CD4-FITC (1/200) (GK1.5), anti-huCD4-PE-Cy7 (1/25) (RPA-T4), anti-TCR-beta-PE-Cy7 (1/100) (H57.59.1, BioLegend), anti-CD44-PerCP-Cy5.5 (1/500) (IM7), CD62L-PE-Cy7 (1/500) (MEL-14), anti-CD8-PerCP-Cy5.5 (1/300) (53-6.7), anti-CD8-APC-eFluor780 (1/300) (53-6.7), anti-CD8-Qdot-655(1/300), anti-Foxp3-APC (1/100) (FJK-16s), anti-Foxp3-FITC (1/100) (FJK-16s), anti-GFP–Alexa Fluor 488 (1/200) (polyclonal, Invitrogen), anti-Ki67-PE (1/50) (B56, BD), anti-Ki67-FITC (1/50) (B56, BD) and anti-Thy1.1-PerCP-Cy5.5 (1/250) (HIS51), anti-IFN-γ-PerCP-Cy5.5 (1/350) (XMG1.2), anti-IL-17A-APC (1/100) (17B7), anti-IL-4-PECy7 (1/100) (BVD6-24G2) (all eBioscience unless indicated otherwise). Intracellular staining for Ki67 and Foxp3 was performed after fixation and permeabilization using the reagents from the eBiosciences Foxp3 staining kit. Intracellular staining for BrdU was performed after Foxp3 staining, using the BrdU staining kit (BD). For intracellular cytokine staining, cells were stimulated for 4 h in complete RPMI in presence of Phorbol myristate acetate (50 ng/ml; Sigma-Aldrich), ionomycin (500 ng/ml; Sigma-Aldrich), and monensin (1/1,000; BD), reagents from the BD cytofix/cytoperm kit were used. Apoptosis was assessed using the Abcam active Caspase-3 FITC Staining Kit.

Biochemical analyses

Anti-dsDNA titers in individual plasma samples were determined by enzyme-linked immunosorbent assay (ELISA). IgE levels were measured with a mouse IgE Ready-SET-Go! ELISA assay (eBioscience). IL-2 concentrations were determined with a mouse IL-2 High Sensitivity ELISA (eBioscience). For *in vitro* stimulation of T_{reg} cells with IL-2, pooled splenic and lymph node cells from *Foxp3*^{Cre} mice were labeled with anti-CD4 microbeads and the $CD4^+$ T cells enriched on an AutoMACS separator (Miltenyi Biotec). Enriched $CD4^+$ cells were stained with anti-CD4-PerCP-Cy5.5 and anti-CD25-PE and YFP^+ T_{reg} cells or YFP^- conventional T cells were purified by cell sorting on a MoFlo FACS machine (Cytomation). T_{reg} cells were plated at 10^5 cells per well in Complete medium with 200 U/well IL-2 (Peprotech). The pan-caspase inhibitor QVD-OPH was added where indicated to prevent Treg apoptosis in the absence of IL-2. After 24 h of culture, T_{reg} cells were recovered in lysis buffer and lysates were separated by SDS-PAGE, then transferred to PVDF membrane for probing with rabbit anti-Mcl-1 (Rockland Immunochemicals), HRPO conjugated anti-rabbit immunoglobulin (Southern Biotech) and development with ECL reagents (GE Healthcare).

Statistics and bioinformatics

Statistical analysis was performed on all data point, excluding only technical failures. No data-points were excluded on the basis of being outliers. All data points shown and used for analysis are biological replicates. Differences in animal survival rates were analyzed using a log rank test (Prism). All other statistical analyses were performed through an ANOVA with Tukey's post-test, followed by individual unpaired two-tailed *t*-test comparisons between two groups, with $P < 0.05$ used as the threshold for statistical significance. Tests were picked in advance of data generation based on experimental design, rather than post-hoc data analysis of data distribution. Data are presented as mean ± s.d., with individual data points overlaid where appropriate.

Prediction of caspase cleavage sites was performed using CASVM[58], using the P14-P10′ scanning window size and allowing aspartic acid and glutamic acid at P1.

Supplementary Material

Refer to Web version on PubMed Central for supplementary material.

Acknowledgments

We thank P. Fink (University of Washington, Seattle, USA) for providing Rag2–GFP-Tg mice backcrossed to the B6 background, L. Hennighausen (National Institutes of Health, Bethesda, USA) for providing *Bcl2l1*^{flox} mice, A. Rudensky (Memorial Sloan-Kettering Cancer Center, New York, USA) for providing *Foxp3*^{GFP}, *Foxp3*^{Cre}, *Foxp3*$^{Thy1.1}$ and *Foxp3*^{DTR} mice, G. Kelly and S. Grabow (Walter and Eliza Hall Institute of Medical Research, Melbourne, Australia) for CreERT2*Mcl1*^{flox} and CreERT2*Bcl2l1*^{flox} mice and *Bcl-2*$^{-/-}$ fetal liver samples, F. Kupresanin, G. Siciliano, G.-F. Dabrowski, K. Humphreys and E. Lanera (Walter and Eliza Hall Institute of Medical Research, Melbourne, Australia) for technical assistance, S. Korsmeyer (Harvard Medical School, Boston, USA) for *Bax*^{flox}*Bak*$^{-/-}$ mice, and A. Kallies (Walter and Eliza Hall Institute of Medical Research, Melbourne, Australia) for critical feedback on the manuscript. This work was supported by grants from the VIB, Marie Curie (TREG to A.L.), European Research Council (IMMUNO to A.L.), Interuniversity Attraction Poles (VII/39 to A.L and P.M.), QSIS (to A.A.F.) and the Australian National Health & Medical Research Council (CDF-1 #637353 to D.H.D.G.). W.P. is funded by Agentschap voor Innovatie door Wetenschap en Technologie. B.C., S.M.S. and S.H.-B. are funded by the Fonds Wetenschappelijk Onderzoek. This work was made possible through Victorian State Government Operational Infrastructure Support and the Australian Government National Health & Medical Research Council Independent Research Institutes Infrastructure Support Scheme.

References

1. Gavin MA, et al. Foxp3-dependent programme of regulatory T-cell differentiation. Nature. 2007; 445:771–775. [PubMed: 17220874]
2. Sakaguchi S, et al. FOXP3^{+} regulatory T cells in the human immune system. Nat Rev Immunol. 2010; 10:490–500. [PubMed: 20559327]
3. Fontenot JD, et al. A function for interleukin 2 in Foxp3-expressing regulatory T cells. Nat Immunol. 2005; 6:1142–1151. [PubMed: 16227984]
4. Chougnet CA, et al. A major role for Bim in regulatory T cell homeostasis. J Immunol. 2011; 186:156–163. [PubMed: 21098226]
5. Siggs OM, et al. Opposing functions of the T cell receptor kinase ZAP-70 in immunity and tolerance differentially titrate in response to nucleotide substitutions. Immunity. 2007; 27:912–926. [PubMed: 18093540]
6. Tian L, et al. Foxp3+ regulatory T cells exert asymmetric control over murine helper responses by inducing Th2 cell apoptosis. Blood. 2011; 118:1845–1853. [PubMed: 21715314]
7. Miyara M, et al. Human FoxP3+ regulatory T cells in systemic autoimmune diseases. Autoimmun Rev. 2011; 10:744–755. [PubMed: 21621000]

8. Lages CS, et al. Functional regulatory T cells accumulate in aged hosts and promote chronic infectious disease reactivation. J Immunol. 2008; 181:1835–1848. [PubMed: 18641321]
9. Raynor J, et al. Homeostasis and function of regulatory T cells in aging. Curr Opin Immunol. 2012; 24:482–487. [PubMed: 22560294]
10. Shimizu J, et al. Stimulation of CD25(+)CD4(+) regulatory T cells through GITR breaks immunological self-tolerance. Nat Immunol. 2002; 3:135–142. [PubMed: 11812990]
11. Baba J, et al. Depletion of radio-resistant regulatory T cells enhances antitumor immunity during recovery from lymphopenia. Blood. 2012; 120:2417–2427. [PubMed: 22806892]
12. Youle RJ, Strasser A. The BCL-2 protein family: opposing activities that mediate cell death. Nat Rev Mol Cell Biol. 2008; 9:47–59. [PubMed: 18097445]
13. Strasser A. The role of BH3-only proteins in the immune system. Nat Rev Immunol. 2005; 5:189–200. [PubMed: 15719025]
14. Huang DC, Strasser A. BH3-Only proteins-essential initiators of apoptotic cell death. Cell. 2000; 103:839–842. [PubMed: 11136969]
15. Zheng L, et al. A novel role of IL-2 in organ-specific autoimmune inflammation beyond regulatory T cell checkpoint: both IL-2 knockout and Fas mutation prolong lifespan of Scurfy mice but by different mechanisms. J Immunol. 2007; 179:8035–8041. [PubMed: 18056343]
16. Ikeda T, et al. Dual effects of TRAIL in suppression of autoimmunity: the inhibition of Th1 cells and the promotion of regulatory T cells. J Immunol. 2010; 185:5259–5267. [PubMed: 20921531]
17. Zhan Y, et al. Defects in the Bcl-2-regulated apoptotic pathway lead to preferential increase of CD25 low Foxp3+ anergic CD4+ T cells. J Immunol. 2011; 187:1566–1577. [PubMed: 21742968]
18. Lindsten T, et al. The combined functions of proapoptotic Bcl-2 family members bak and bax are essential for normal development of multiple tissues. Mol Cell. 2000; 6:1389–1399. [PubMed: 11163212]
19. Wang X, et al. Preferential control of induced regulatory T cell homeostasis via a Bim/Bcl-2 axis. Cell Death Dis. 2012; 3:e270. [PubMed: 22318539]
20. Liu N, et al. Selective impairment of CD4+CD25+Foxp3+ regulatory T cells by paclitaxel is explained by Bcl-2/Bax mediated apoptosis. Int Immunopharmacol. 2011; 11:212–219. [PubMed: 21115120]
21. Tischner D, et al. Defective cell death signalling along the Bcl-2 regulated apoptosis pathway compromises Treg cell development and limits their functionality in mice. J Autoimmun. 2012; 38:59–69. [PubMed: 22257939]
22. Motoyama N, et al. Massive cell death of immature hematopoietic cells and neurons in Bcl-x-deficient mice. Science. 1995; 267:1506–1510. [PubMed: 7878471]
23. Ma A, et al. Bclx regulates the survival of double-positive thymocytes. Proc Natl Acad Sci USA. 1995; 92:4763–4767. [PubMed: 7761398]
24. Rubtsov YP, et al. IL-10 produced by regulatory T cells contributes to their suppressor function by limiting inflammation at environmental interfaces. Immunity. 2008; 28:546–558. [PubMed: 18387831]
25. Wagner KU, et al. Conditional deletion of the Bcl-x gene from erythroid cells results in hemolytic anemia and profound splenomegaly. Development. 2000; 127:4949–4958. [PubMed: 11044408]
26. Vikstrom I, et al. Mcl-1 is essential for germinal center formation and B cell memory. Science. 2010; 330:1095–1099. [PubMed: 20929728]
27. Schlenner SM, et al. Fate mapping reveals separate origins of T cells and myeloid lineages in the thymus. Immunity. 2010; 32:426–436. [PubMed: 20303297]
28. Dzhagalov I, et al. The anti-apoptotic Bcl-2 family member Mcl-1 promotes T lymphocyte survival at multiple stages. J Immunol. 2008; 181:521–528. [PubMed: 18566418]
29. Opferman JT, et al. Development and maintenance of B and T lymphocytes requires antiapoptotic MCL-1. Nature. 2003; 426:671–676. [PubMed: 14668867]
30. Strasser A, et al. Deciphering the rules of programmed cell death to improve therapy of cancer and other diseases. EMBO J. 2011; 30:3667–3683. [PubMed: 21863020]

31. Bouillet P, et al. Proapoptotic Bcl-2 relative Bim required for certain apoptotic responses, leukocyte homeostasis, and to preclude autoimmunity. Science. 1999; 286:1735–1738. [PubMed: 10576740]
32. Gray DH, et al. The BH3-only proteins Bim and Puma cooperate to impose deletional tolerance of organ-specific antigens. Immunity. 2012; 37:451–462. [PubMed: 22960223]
33. Boyman O, et al. Selective stimulation of T cell subsets with antibody-cytokine immune complexes. Science. 2006; 311:1924–1927. [PubMed: 16484453]
34. Bautista JL, et al. Intraclonal competition limits the fate determination of regulatory T cells in the thymus. Nat Immunol. 2009; 10:610–617. [PubMed: 19430476]
35. Liston A, Rudensky AY. Thymic development and peripheral homeostasis of regulatory T cells. Curr Opin Immunol. 2007; 19:176–185. [PubMed: 17306520]
36. Tai X, et al. Foxp3 is pro-apoptotic and lethal to developing regulatory T cells unless counterbalanced by cytokine survival signals. Immunity. 2013 (in the press).
37. Walker LS. CD4+ CD25+ Treg: divide and rule? Immunology. 2004; 111:129–137. [PubMed: 15027897]
38. McNeill A, et al. Partial depletion of CD69low-expressing natural regulatory T cells with the anti-CD25 monoclonal antibody PC61. Scand J Immunol. 2007; 65:63–69. [PubMed: 17212768]
39. Suffner J, et al. Dendritic cells support homeostatic expansion of Foxp3+ regulatory T cells in Foxp3.LuciDTR mice. J Immunol. 2010; 184:1810–1820. [PubMed: 20083650]
40. Guy CS, et al. Distinct TCR signaling pathways drive proliferation and cytokine production in T cells. Nat Immunol. 2013; 14:262–270. [PubMed: 23377202]
41. Khan WN. B cell receptor and BAFF receptor signaling regulation of B cell homeostasis. J Immunol. 2009; 183:3561–3567. [PubMed: 19726767]
42. Carrette F, Surh CD. IL-7 signaling and CD127 receptor regulation in the control of T cell homeostasis. Semin Immunol. 2012; 24:209–217. [PubMed: 22551764]
43. Dummer W, et al. Autologous regulation of naive T cell homeostasis within the T cell compartment. J Immunol. 2001; 166:2460–2468. [PubMed: 11160306]
44. Gorelik L, et al. Normal B cell homeostasis requires B cell activation factor production by radiation-resistant cells. J Exp Med. 2003; 198:937–945. [PubMed: 12975458]
45. Wing K, et al. CTLA-4 control over Foxp3+ regulatory T cell function. Science. 2008; 322:271–275. [PubMed: 18845758]
46. Liston A, et al. Dicer-dependent microRNA pathway safeguards regulatory T cell function. J Exp Med. 2008; 205:1993–2004. [PubMed: 18725526]
47. Takeuchi O, et al. Essential role of BAX, BAK in B cell homeostasis and prevention of autoimmune disease. Proc Natl Acad Sci USA. 2005; 102:11272–11277. [PubMed: 16055554]
48. Caton ML, et al. Notch-RBP-J signaling controls the homeostasis of CD8-dendritic cells in the spleen. J Exp Med. 2007; 204:1653–1664. [PubMed: 17591855]
49. Fontenot JD, et al. Regulatory T cell lineage specification by the forkhead transcription factor foxp3. Immunity. 2005; 22:329–341. [PubMed: 15780990]
50. Liston A, et al. Differentiation of regulatory Foxp3+ T cells in the thymic cortex. Proc Natl Acad Sci USA. 2008; 105:11903–11908. [PubMed: 18695219]
51. Mombaerts P, et al. RAG-1-deficient mice have no mature B and T lymphocytes. Cell. 1992; 68:869–877. [PubMed: 1547488]
52. Yu W, et al. Continued RAG expression in late stages of B cell development and no apparent re-induction after immunization. Nature. 1999; 400:682–687. [PubMed: 10458165]
53. Srinivas S, et al. Cre reporter strains produced by targeted insertion of EYFP and ECFP into the ROSA26 locus. BMC Dev Biol. 2001; 1:4. [PubMed: 11299042]
54. Buch T, et al. A Cre-inducible diphtheria toxin receptor mediates cell lineage ablation after toxin administration. Nat Methods. 2005; 2:419–426. [PubMed: 15908920]
55. Seibler J, et al. Rapid generation of inducible mouse mutants. Nucleic Acids Res. 2003; 31:e12. [PubMed: 12582257]
56. Kim JM, et al. Regulatory T cells prevent catastrophic autoimmunity throughout the lifespan of mice. Nat Immunol. 2007; 8:191–197. [PubMed: 17136045]

57. Létourneau S, et al. IL-2/anti-IL-2 antibody complexes show strong biological activity by avoiding interaction with IL-2 receptor alpha subunit CD25. Proc Natl Acad Sci USA. 2010; 107:2171–2176. [PubMed: 20133862]

58. Wee LJ, et al. CASVM: web server for SVM-based prediction of caspase substrates cleavage sites. Bioinformatics. 2007; 23:3241–3243. [PubMed: 17599937]

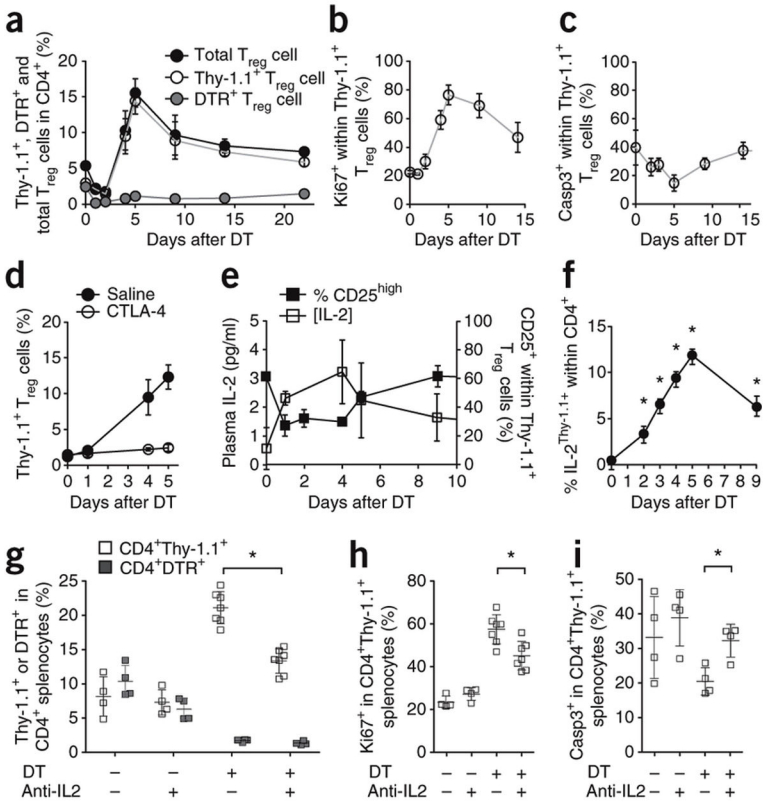

Figure 1.

Homeostatic expansion of T_{reg} cells is driven by increased production of IL-2. (**a**) Percentages of DTR^+ T_{reg} cells $Thy1.1^+$ T_{reg} cells and total T_{reg} cells in *Foxp3*$^{Thy1.1/DTR}$ females depleted of $Foxp3^{DTR+}$ T_{reg} cells on day 0. Blood leukocytes were assessed on indicated days (*n=4,3,7,3,4,4,4,4* mice). (**b**,**c**) Proliferation rate (**b**; percentage $Ki67^+$) and apoptosis rate (**c**; percentage activated caspase 3^+) of $Thy1.1^+$ T_{reg} cells, after DT treatment of *Foxp3*$^{Thy1.1/DTR}$ females on day 0. (**d**) Percentages of $Thy1.1^+$ T_{reg} cells in peripheral blood after DT treatment of saline-treated (*n=3,3,3* mice/group) or CTLA4-Ig–treated *Foxp3*$^{Thy1.1/DTR}$ female mice (*n=3,3,3* mice/group). (**e**) Plasma IL-2 (left axis, *n=27,3,3,12,14* mice/group) and surface CD25 expression on $Thy1.1^+$ T_{reg} cells (right axis, *n=4,3,7,3,4,4* mice/group) from days 0 to 15 for female *Foxp3*$^{Thy1.1/DTR}$ mice depleted of $Foxp3^{DTR+}$ T_{reg} cells (**f**) Proportion of $Thy1.1^+$ (reporter for IL-2) cells within the $CD4^+Foxp3^-$ population after DT injection of *Foxp3*$^{+/DTR}$*.IL2-Thy1.1* mice. (**g**) *Foxp3*$^{Thy1.1/DTR}$ mice were depleted of DTR^+ T_{reg} cells and injected daily with an IL-2 blocking antibody (a-IL2) or an immunoglobulin isotype-matched control antibody. Splenocytes were analyzed on day 6 for the percentages of DTR^+ and $Thy1.1^+$ T_{reg} cells, with or without T_{reg} cell depletion (DT treatment) and with or without anti–IL-2 treatment (*n=4,4,7,7* mice/group). (**h,i**) Proliferation rate (**h**; percentage $Ki67^+$) and apoptosis rate (**i**; activated caspase-3^+) of $Thy1.1^+$ regulatory T cells, with or without DT treatment and with or without anti-IL-2 treatment (*n=4*). (**a–i**) Mean ± s.d., $*P < 0.05$, t-test. Data are representative of 3(**a–f**) and 2 (**g–i**) independent experiments.

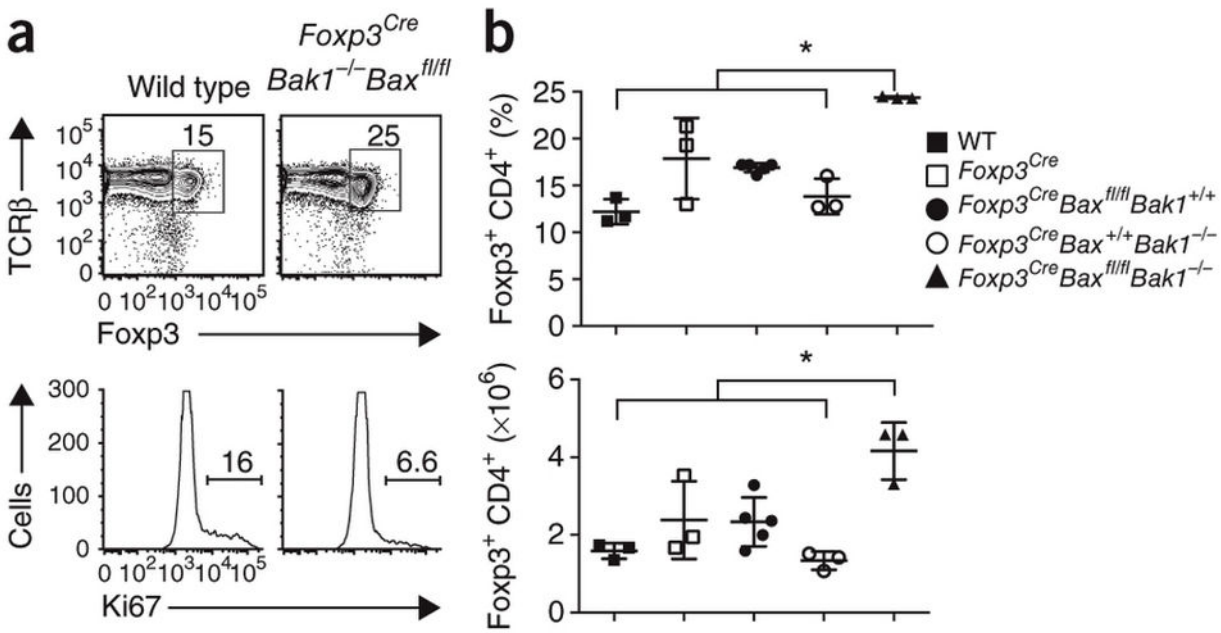

Figure 2.

The intrinsic apoptosis pathway is required to restrain T_{reg} cell numbers to homeostatic levels. (**a**) Representative flow profiles (TCRβ versus Foxp3 gated on $CD4^+$ cells, Ki67 histograms gated on $Foxp3^+$ $CD4^+$ cells) for wild-type, *Foxp3*^{Cre}*Bak*$^{-/-}$*Bax*$^{fl/fl}$ mice and control littermates at 6–8 weeks of age. Numbers in plots indicate (top) the percentage of $Foxp3^+TCR\beta^+$ regulatory T cells and (bottom) the fraction of proliferating $Foxp3^+CD4^+$ cells ($Ki67^+$). (**b**) Average percentages and absolute numbers (mean ± s.d.) of splenic $Foxp3^+$ T_{reg} cells in wt, *Foxp3*^{Cre}*Bak*$^{-/-}$*Bax*$^{fl/fl}$ mice and control littermates at 6–8 weeks of age (*n=3,3,5,3* mice/group). (**a–b**) Data from one experiment representative of three are shown. Mean ± s.d., **P* < 0.05, t-test.

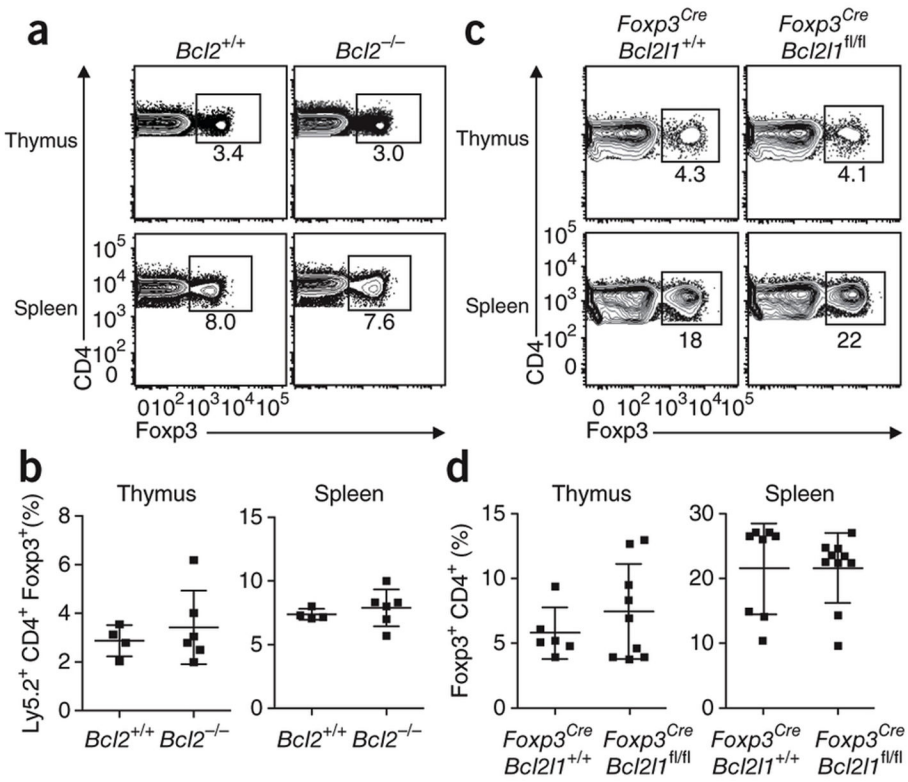

Figure 3.

Regulatory T cell survival is independent of Bcl-2 and Bcl-x_L. (**a**) C57BL/6.Ly5.1 (Ly5.1) chimeras reconstituted with a 50:50 mixture of hematopoietic precursors from wild-type Ly5.1 and either *Bcl2*$^{+/+}$ or *Bcl2*$^{-/-}$ mice, analyzed 8–12 weeks later. Gates show the percentage of Ly5.2$^+$CD4$^+$Foxp3$^+$ cells recovered from the thymus or spleen. (**b**) Average percentages (mean ± s.d.) of Ly5.2$^+$CD4$^+$Foxp3$^+$ cells recovered from the thymus and spleen of the same mixed hematopoietic chimeras reconstituted with precursors from either wild-type (*Bcl2*$^{+/+}$) or *Bcl2*$^{-/-}$ mice (*n= 4,6* mice/group). (**a,b**) Data from one experiment representative of three are shown. (**c**) Representative flow profiles of CD4 versus Foxp3 gated on CD4$^+$ cells from *Foxp3*^{Cre}*Bcl2l1*$^{wt/wt}$ and *Foxp3*^{Cre}*Bcl2l1*$^{fl/fl}$ mice. Gates show the percentage of CD4$^+$Foxp3$^+$ cells recovered from the thymus or spleen. (**d**) Average percentages (mean ± s.d.) of CD4$^+$Foxp3$^+$ T_{reg} cells in the thymus and spleen of *Foxp3*^{Cre}*Bcl2l1*$^{wt/wt}$ and *Foxp3*^{Cre}*Bcl2l1*$^{fl/fl}$ siblings at 6–8 weeks of age (*n* = 6,9 respectively). (**c,d**) Data pooled from three independent experiments are shown.

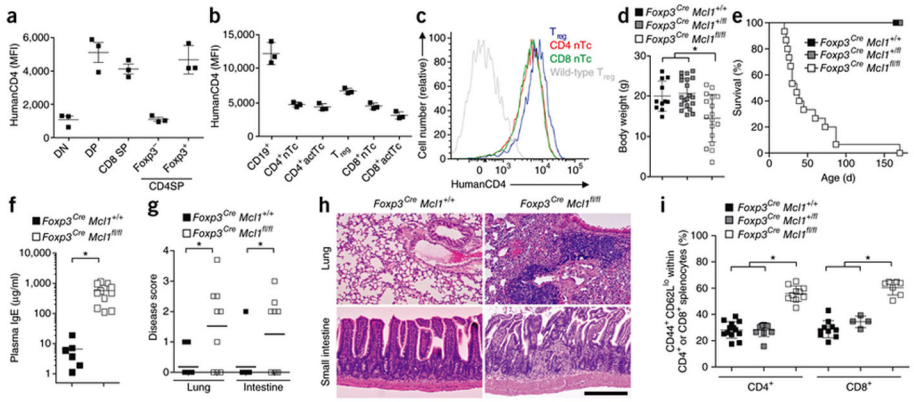

Figure 4.

Spontaneous fatal immunopathology after T_{reg} cell–specific deletion of Mcl-1. (**a**) HuCD4 reporter for Mcl-1 expression was measured in lymphocyte subsets in *Cd127*^{Cre}*Mcl1*$^{wt/fl\text{-}huCD4}$ female mice, 6–8 weeks of age. Average huCD4 reporter MFI in CD4$^-$CD8$^-$ (DN), CD4$^+$CD8$^+$ (DP) and single positive (SP) thymocytes, the latter subdivided into CD4$^-$CD8$^+$ SP, conventional CD4$^+$CD8$^-$ SP and CD4$^+$CD8$^-$ Foxp3$^+$ SP (*n* = 3 mice/group). (**b**) Average huCD4 reporter MFI in splenic CD19$^+$ B cells, naïve conventional CD4$^+$ (CD4$^+$ nTc), activated conventional CD4$^+$ (CD4$^+$ actTc), Foxp3$^+$ T_{reg} cells, naive conventional CD8$^+$ (CD8$^+$ nTc) and activated conventional CD8$^+$ T cells (CD8$^+$ actTc) (*n* = 3 mice/group). (**c**) Representative histogram of huCD4 reporter MFI in naive conventional CD4$^+$ (CD4$^+$ nTc), Foxp3$^+$ T_{reg} cells and naive conventional CD8$^+$ (CD8$^+$ nTc), with control huCD4 staining in wild-type Foxp3$^+$ T_{reg} cells. (**a–c**) Data from one experiment representative of three. (**d**) Weights of male *Foxp3*^{Cre}*Mcl1*$^{wt/wt}$, *Foxp3*^{Cre}*Mcl1*$^{wt/fl}$ and *Foxp3*^{Cre}*Mcl1*$^{fl/fl}$ littermates at 6–8 weeks of age (*n=11,20,16* mice/group). (**e**) Survival curve for male *Foxp3*^{Cre}*Mcl1*$^{wt/wt}$, *Foxp3*^{Cre}*Mcl1*$^{wt/fl}$ and *Foxp3*^{Cre}*Mcl1*$^{fl/fl}$ littermates (*n=16,18,18* mice/group)). (**f**) Plasma IgE levels in male *Foxp3*^{Cre}*Mcl1*$^{wt/wt}$ and *Foxp3*^{Cre}*Mcl1*$^{fl/fl}$ littermates at 4–8 weeks of age (*n=6,12* mice/group). (**g**,**h**) Average disease score (**g**) and representative histology (**h**; scale bar, 200 μm) of the lungs and small intestine of male *Foxp3*^{Cre}*Mcl1*$^{wt/wt}$ and *Foxp3*^{Cre}*Mcl1*$^{fl/fl}$ littermates at 4–8 weeks of age (*n=11, 9* mice/group). (**i**) Average percentage of CD44$^+$CD62L^{low} activated cells within CD4$^+$ and CD8$^+$ splenic T cells in *Foxp3*^{Cre}*Mcl1*$^{wt/wt}$, *Foxp3*^{Cre}*Mcl1*$^{wt/fl}$ and *Foxp3*^{Cre}*Mcl1*$^{fl/fl}$ littermates at 6–8 weeks of age (*n=12,9,11,10,4,d8* mice/group). (**d–i**) Data pooled from 3 experiments. Mean ± s.d., * $P < 0.05$, t-test.

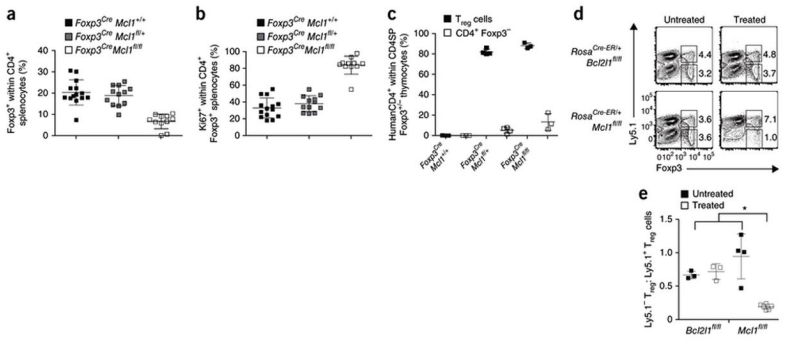

Figure 5.

Mcl-1 is required for T_{reg} cell survival. (**a**) Average percentages of Foxp3$^+$ T_{reg} cells within splenic CD4$^+$ T cells in male *Foxp3^{Cre}Mcl1$^{wt/wt}$*, *Foxp3^{Cre}Mcl1$^{wt/fl}$* and *Foxp3^{Cre}Mcl1$^{fl/fl}$* littermates at 6–8 weeks of age (*n=14,12,11* mice/group). (**b**) Average percentages of Ki67$^+$ cells within splenic Foxp3$^+$ T_{reg} cells in *Foxp3^{Cre}Mcl1$^{wt/wt}$*, *Foxp3^{Cre}Mcl1$^{wt/fl}$* and *Foxp3^{Cre}Mcl1$^{fl/fl}$* littermates at 6–8 weeks of age (*n=14,12,11* mice/group). (**a,b**) Data pooled from 3 experiments. **c**) Expression of the huCD4 reporter for excision of *Mcl1* in Foxp3$^+$ and Foxp3$^-$ cells in male *Foxp3^{Cre}Mcl1$^{fl/fl}$* mice (*n=3,4,3* mice/group). Data from one experiment representative of three. (**d**) Ly5.1 versus Foxp3 expression on lymph node cells from mixed chimeras with *Mcl1*$^{fl/fl}$ or *Bcl2l1*$^{fl/fl}$ Ly5.2 donor compartments analyzed 3 d after treatment with tamoxifen or vehicle control. Gates display the fraction of T_{reg} cells arising from (top) wildtype Ly5.1$^+$ and (bottom) *Mcl1*$^{fl/fl}$ or *Bcl2l1*$^{fl/fl}$ Ly5.1$^-$ cells. Plots are representative of 3 experiments, each with *n* = 3 mice/group. (**e**) Ratios of Ly5.1$^+$ to Ly5.1$^-$ CD4$^+$Foxp3$^+$ lymph node cells in mixed chimeras with the indicated Ly5.2$^+$ donor compartment 3 d after treatment with tamoxifen or vehicle (*n=3,3,4,6* mice/group). Data from one experiment representative of three is shown. Mean ± s.d., **P* < 0.05, t-test.

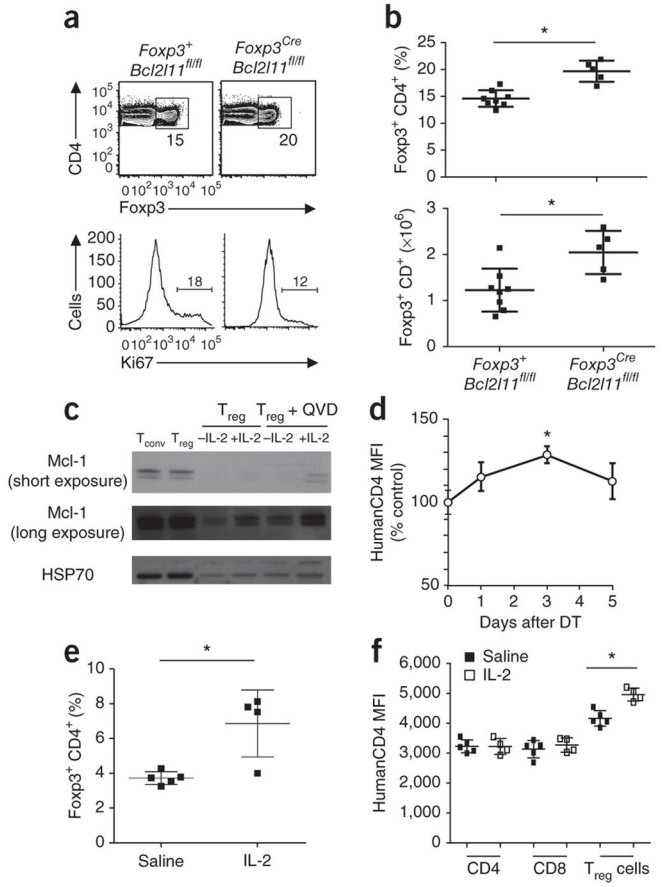

Figure 6.

Regulation of Mcl-1 in T_{reg} cells by Bim and IL-2. (**a**) Representative flow cytometric profiles for CD4 vs Foxp3 gated on $CD4^+$ cells (gates indicate fraction of T_{reg} cells within $CD4^+$ lymph node cells) and Ki67 histograms gated on $Foxp3^+CD4^+$ cells (gate indicates the fraction of proliferating T_{reg} cells) for *Foxp3*^{wt}*Bcl2l11*$^{fl/fl}$ and *Foxp3*^{Cre}*Bcl2l11*$^{fl/fl}$ littermates at 6–8 weeks of age. (**b**) Average percentages and absolute number of $CD4^+Foxp3^+$ T_{reg} cells from pooled lymph nodes of *Foxp3*^{wt}*Bcl2l11*$^{fl/fl}$ and *Foxp3*^{Cre}*Bcl2l11*$^{fl/fl}$ littermates (*n=8,5* mice/group). Data from one experiment representative of three are shown. (**c**) Immunoblot analysis of Mcl-1 expression in *ex vivo* isolated conventional T cells (T_{conv}) or T_{reg} cells, or T_{reg} cells cultured overnight with or without IL-2, in the absence or presence of QVD-OPH (a broad spectrum caspase inhibitor used to prevent apoptosis in the absence of IL-2). Data from one experiment representative of three are shown. (**d**) *Cd127*^{Cre}*Mcl1*$^{wt/fl\text{-}huCD4}$*Foxp3*$^{wt/DTR}$ females were depleted of $Foxp3^{DTR+}$ T_{reg} cells on day 0 and huCD4 (*Mcl1* reporter) expression was measured in $Foxp3^+$ T_{reg} cells during the expansion phase. MFI was normalized to T_{reg} cells from *Cd127*^{Cre}*Mcl1*$^{wt/fl\text{-}huCD4}$*Foxp3*^{wt} mice (*n=4* mice/group). Data from one experiment representative of two are shown. (**e**) *Cd127*^{Cre}*Mcl1*$^{wt/fl\text{-}huCD4}$ mice were injected with IL-2-anti-IL-2 antibody complexes or saline and on day 2 were measured for $CD4^+Foxp3^+$ T_{reg}

cell expansion in the peripheral blood and **f,** expression of huCD4 reporter for *Mcl1* expression (*n=5,4* mice/group). Mean ± s.d., * $P < 0.05$, t-test.